

## Rapid prediction of long-term deflections in composite frames

Umesh Pendharkar<sup>1a</sup>, K.A. Patel<sup>2b</sup>, Sandeep Chaudhary<sup>\*3</sup> and A.K. Nagpal<sup>2c</sup>

<sup>1</sup> School of Engineering and Technology, Vikram University, Ujjain 456010, India

<sup>2</sup> Civil Engineering Department, Indian Institute of Technology Delhi, New Delhi 110016, India

<sup>3</sup> Civil Engineering Department, Malaviya National Institute of Technology Jaipur, Jaipur 302017, India

(Received April 18, 2014, Revised August 10, 2014, Accepted August 21, 2014)

**Abstract.** Deflection in a beam of a composite frame is a serviceability design criterion. This paper presents a methodology for rapid prediction of long-term mid-span deflections of beams in composite frames subjected to service load. Neural networks have been developed to predict the inelastic mid-span deflections in beams of frames (typically for 20 years, considering cracking, and time effects, i.e., creep and shrinkage in concrete) from the elastic moments and elastic mid-span deflections (neglecting cracking, and time effects). These models can be used for frames with any number of bays and stories. The training, validating, and testing data sets for the neural networks are generated using a hybrid analytical-numerical procedure of analysis. Multilayered feed-forward networks have been developed using sigmoid function as an activation function and the back propagation-learning algorithm for training. The proposed neural networks are validated for an example frame of different number of spans and stories and the errors are shown to be small. Sensitivity studies are carried out using the developed neural networks. These studies show the influence of variations of input parameters on the output parameter. The neural networks can be used in every day design as they enable rapid prediction of inelastic mid-span deflections with reasonable accuracy for practical purposes and require computational effort which is a fraction of that required for the available methods.

**Keywords:** composite frames; cracking; creep; deflection; neural networks

### 1. Introduction

Steel-concrete composite beam (Fig. 1) is an integral part of a composite frame. Maximum deflection in a beam of a frame is a design criterion and occurs generally at or close to the mid-span of the beam. The application of loads on the frames can result in instantaneous increase in the tensile stresses of the top fibers of the concrete slab in the negative moment region. An instantaneous cracking of concrete takes place when these stresses exceed the tensile strength of the concrete. The effective section of the composite beam after cracking of concrete reduces from the composite section to the bare steel section and this may cause change in mid-span deflections

---

\*Corresponding author, Ph.D., E-mail: [schaudhary.ce@mnit.ac.in](mailto:schaudhary.ce@mnit.ac.in); [sandeep.nitjaipur@gmail.com](mailto:sandeep.nitjaipur@gmail.com)

<sup>a</sup> Ph.D., E-mail: [umeshpendharkar@gmail.com](mailto:umeshpendharkar@gmail.com)

<sup>b</sup> M.Tech., E-mail: [iitd.kashyap@gmail.com](mailto:iitd.kashyap@gmail.com)

<sup>c</sup> Ph.D., E-mail: [aknagpal@civil.iitd.ac.in](mailto:aknagpal@civil.iitd.ac.in)

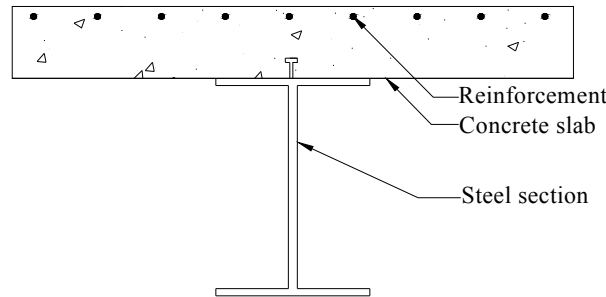


Fig. 1 Cross-section of composite beam

of the beam. There may be further change in mid-span deflection due to the time effects of creep and shrinkage in concrete. The appropriate prediction of mid-span deflections after moment redistribution owing to the cracking and time effects in concrete is therefore important from serviceability considerations. Methods are available in the literature for the same (Ghali *et al.* 2002). These methods are based either on incremental or iterative approach. Both the approaches require a computational effort, which is significantly more than that required for the elastic analysis (neglecting instantaneous cracking and time effects in concrete). The computational effort required may be huge for large composite framed structures. The technique of neural network can be employed to drastically reduce the computational effort in such cases.

Neural networks have been extensively applied in the field of structural engineering. Some of the applications of neural networks in the field of structural engineering include determination of wind induced pressures on gable roof (Kwatra *et al.* 2002), development of performance evaluation systems for concrete bridges (Kawamura *et al.* 2004, Feng *et al.* 2004), prediction of the creep response of a rotating composite disc operating at elevated temperature (Gupta *et al.* 2007), prediction of damage detection in reinforced concrete framed buildings after earthquake (Kanwar *et al.* 2007), estimation of ultimate pure bending of steel circular tubes (Shahin and Elchanakani 2008), static model identification (Kim *et al.* 2009), optimal seismic design of steel structures (Gholizadeh and Salajegheh 2010), response prediction of offshore floating structure (Uddin *et al.* 2012), structural health monitoring (Min *et al.* 2012, Kaloop and Kim 2014) and prediction of the deflection of high strength self compacting concrete deep beams (Mohammadhassani *et al.* 2013a, b). These studies reveal the strength of neural networks in predicting the solutions of different structural engineering problems.

Further, neural networks have been applied to predict the various design quantities in steel-concrete composite structures including bending moments and deflections in continuous composite beams considering concrete cracking (Chaudhary *et al.* 2007a, 2014), bending moments and deflections in continuous composite beams considering cracking and time effects in concrete (Pendharkar *et al.* 2007, 2010), deflections in composite bridges considering flexibility of shear connectors, concrete cracking and shear lag effect (Tadesse *et al.* 2012, Gupta *et al.* 2013), and moments in composite frames considering cracking and time effects in concrete (Pendharkar *et al.* 2011).

In this paper, neural networks have been developed for rapid prediction of the inelastic mid-span deflections,  $D^i$  (considering the instantaneous cracking and time effects in concrete) from the elastic mid-span deflections,  $D^e$  (neglecting the instantaneous cracking and time effects in concrete).  $D^e$ , in turn, can be obtained from any of the readily available software. These neural

networks enable rapid estimation of inelastic deflections of the beam spans and require a computational effort that is a fraction of that required for the methods available in the literature. The proposed neural networks have been verified for a number of example frames. The errors are shown to be small for practical purposes. Sensitivity analysis is carried out to study the influence of variations of input parameters on the output parameter.

## 2. Analysis of composite frames

For generalized and efficient neural networks, a huge number of training data sets are required; for the generation of which, a highly efficient method is desirable. A hybrid analytical-numerical procedure (Chaudhary *et al.* 2007b) has therefore been adopted which takes into account the nonlinear effects of cracking in composite beams near interior joints and time-dependent effects of creep and shrinkage composite beams of composite frames. The procedure is analytical at the element level and numerical at the structural level. A cracked span length composite beam element, consisting of two cracked zones (concrete being cracked due to higher tensile stresses) of length  $x_A$  and  $x_B$  at the ends A and B respectively and an uncracked zone in the middle (Fig. 2), has been used in the procedure (Chaudhary *et al.* 2007b, c). For a completely cracked beam element of total length  $L$ ,  $x_A$  and  $x_B$  would be equal to  $L/2$  and for a completely uncracked beam element  $x_A$  and  $x_B$  would be equal to zero. Slip at the interface of the concrete slab and the steel section is neglected assuming that shear connectors are at a sufficiently close spacing. The effect of slip has been reported to be small in comparison to the time-dependent deformations (Wang *et al.* 2011).

The analysis in the hybrid procedure is carried out in two parts. In the first part, an instantaneous analysis is carried out using an iterative method. In the second part, a time-dependent analysis is carried out by dividing the time into a number of time intervals to take into account the progressive nature of cracking of concrete (Fig. 3). As shown in figure, crack

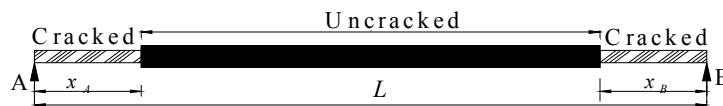


Fig. 2 Cracked span length beam element

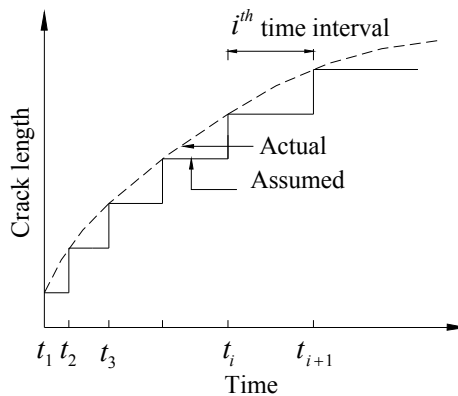


Fig. 3 Progressive nature of cracking

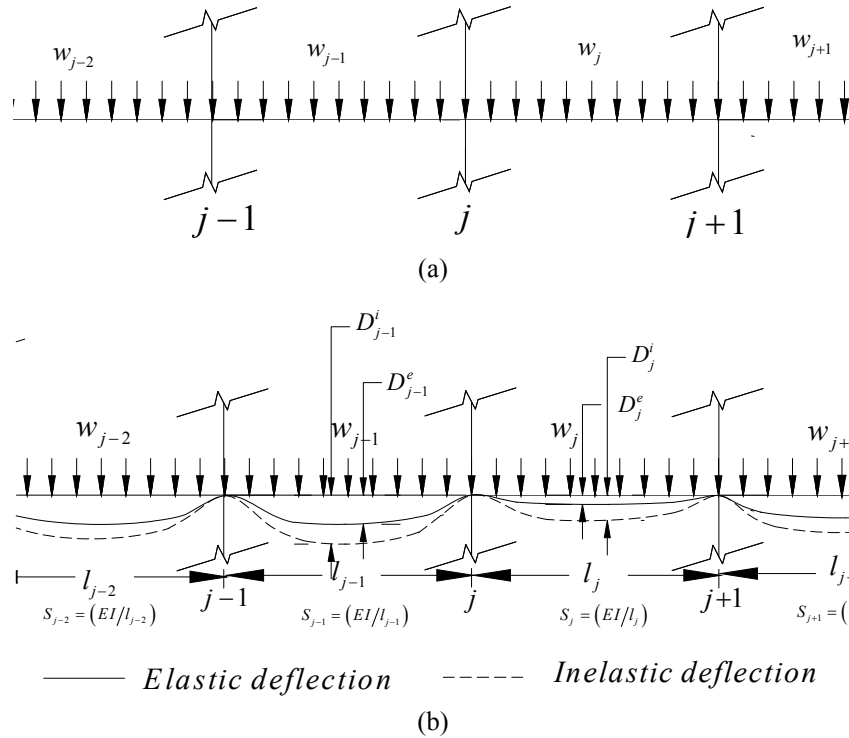


Fig. 4 (a) An intermediate floor of a frame with the loading; and (b) natures of elastic and inelastic deflections

lengths are assumed to be constant in a time-interval and revised at the end of each time interval. The aged-adjusted effective modulus method, AEMM (Bazant 1972) is used for predicting the creep and shrinkage effects which has been used earlier also for other type of composite frames (Sharma *et al.* 2003). CEB-FIP MC 90 (1993) is used for predicting the short term as well as time-dependent properties of the concrete.

The procedure has been validated by comparison with the experimental, analytical, and finite element method results (Chaudhary *et al.* 2007b).

### 3. Structural parameters

As stated earlier in Section 1, instantaneous cracking in composite beams of frames occurs in the end portions (where negative moments occur) when tensile stresses are higher than the tensile strength of concrete. This instantaneous cracking may further progress due to time effects. The elastic mid-span deflection,  $D^e$  at an instantaneous stage gets redistributed owing to cracking and there is a further change in mid-span deflection in beams of frames owing to time effects of creep and shrinkage leading to  $D^i$  at a final stage (typically 20 years).

The change in the mid-span deflection of a span  $j$  of a beam in a frame may be expressed in terms of a ratio designated as inelastic deflection ratio,  $\delta_j = \{(D_j^i - D_j^e) / D_j^{eq}\}$  (where  $D_j^{eq} = M^{cr} l_j^2 / 32EI$  is the mid-span deflection of span  $j$  of a beam in a frame with both ends assumed to

be fixed and subjected to uniformly distributed cracking load,  $w^{cr}$ , where,  $w^{cr}$  that is the minimum load at which the cracking takes place in the beam). This ratio is considered as the output parameter for the neural networks.

Consider an intermediate floor of a frame with the loading (Fig. 4(a)). The nature of elastic and inelastic deflections of a span,  $j$  of a beam of an intermediate floor of a frame is shown in the Fig. 4(b).

Since cracking, creep, and shrinkage effects, in the type of frames being considered, are confined to beams only, it may be postulated based on the studies on the composite beams (Pendharkar *et al.* 2010), that in order to establish inelastic mid-span deflection of a span,  $j$  of a beam in a frame, cracking at beam-column joints,  $j$  and  $j+1$  of the span, needs to be considered. Keeping this in view, the following input parameters for an internal span  $j$  with end joints  $j$  and  $j+1$ , of a frame are identified as:

1. Cracking moment ratio on the left side of joint  $j$ ,  $R_j^l (= M^{cr}/M_j^{e,l})$ ,
2. Cracking moment ratio on the right side of joint  $j$ ,  $R_j^r (= M^{cr}/M_j^{e,r})$ ,
3. Cracking moment ratio on the left side of joint  $j+1$ ,  $R_{j+1}^l (= M^{cr}/M_{j+1}^{e,l})$ ,
4. Cracking moment ratio on the right side of joint  $j+1$ ,  $R_{j+1}^r (= M^{cr}/M_{j+1}^{e,r})$ ,
5. Cracking moment ratio on the right side of joint  $j-1$ ,  $R_{j-1}^r (= M^{cr}/M_{j-1}^{e,r})$ ,
6. Cracking moment ratio on the left side of joint  $j+2$ ,  $R_{j+2}^l (= M^{cr}/M_{j+2}^{e,l})$ ,
7. Stiffness ratio of adjacent spans at joint  $j$ ,  $S_{j-1}/S_j$  ( $S_j = EI^{un}/l_j$ , where  $E$  = modulus of elasticity of concrete, and  $I^{un}$  = transformed moment inertia of composite section about top fiber, the reference axis),
8. Stiffness ratio of adjacent spans at joint  $j+1$ ,  $S_j/S_{j+1}$ ,
9. Load ratio of the adjacent spans at joint  $j$ ,  $w_{j-1}/w_j$ ,
10. Load ratio of the adjacent spans at joint  $j+1$ ,  $w_j/w_{j+1}$ ,
11. Composite inertia ratio,  $I^{cr}/I^{un}$  ( $I^{cr}$  = transformed moment of inertia of steel section and reinforcement about top fiber, the reference axis),
12. Age of loading,  $t_0$ ,
13. Grade of concrete,  $G_r$ .

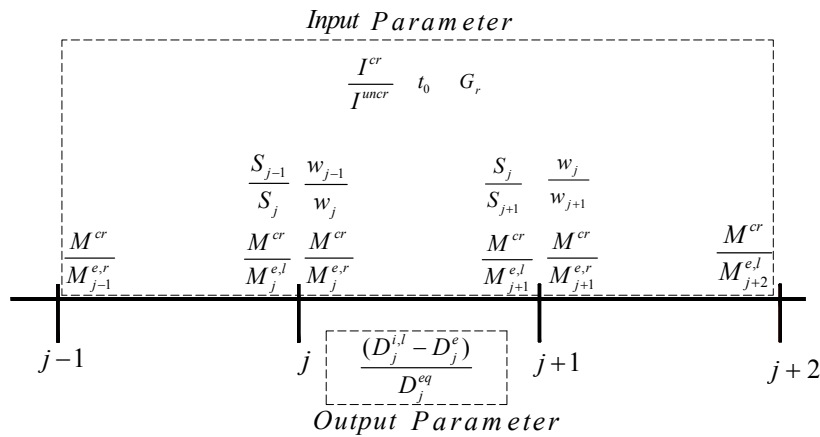


Fig. 5 Schematic representation of input and output parameters

These input parameters are schematically shown in Fig. 5. The practical ranges for the different structural parameters are considered as:  $R_j^l, R_j^r, R_{j+1}^l, R_{j+1}^r, R_{j-1}^r, R_{j+2}^r = 0.25 - 4.0$ ;  $S_{j-1}/S_j, S_j/S_{j+1} = 0.25 - 4.0$ ;  $w_{j-1}/w_j, w_j/w_{j+1} = 0.25 - 4.0$ ;  $I^{cr}/I^{un} = 0.38 - 0.54$ ;  $t_0 = 7 \text{ days} - 21 \text{ days}$ ;  $Gr = 20 \text{ N/mm}^2 - 40 \text{ N/mm}^2$ .

It may be noted that the ratio of beam stiffness to column stiffness is not taken as an input parameter; since in the output parameter  $\delta_j$ , both  $D_j^e$  and  $D_j^i$  may be assumed to be affected approximately to the same degree by variation in beam to column stiffness.

All the neural networks are trained for a particular value of relative humidity,  $RH (= 85\%)$ . The output parameter for other values of relative humidity can be estimated in a manner similar to that explained by Pendharkar *et al.* (2011) for bending moments.

#### 4. Configuration of neural network models

Artificial neural network is a computational model inspired by a human's central nervous systems of the brain which is capable of machine learning and pattern recognition. A neural network comprising processing elements, input-hidden-output layers, weighting factors, activation function and learning function. Neural network is presented as a system of neurons interconnected between input, hidden and output layers which can compute from inputs and outputs. Raw information has been fed by input neurons and made connections between input and hidden neurons through weights and biases and finally output neurons give the information using connections between hidden and output neurons. The neural networks chosen in the present study are multilayered feed-forward networks with neurons in all the layers fully connected in feed forward manner (Fig. 6). The back propagation learning algorithm is used for training and Sigmoid function is used as an activation function as follow

$$f(x) = \frac{1}{1 + e^{-x}} \quad (1)$$

Neural networks are widely used for last two decades owing to their characteristics like pattern

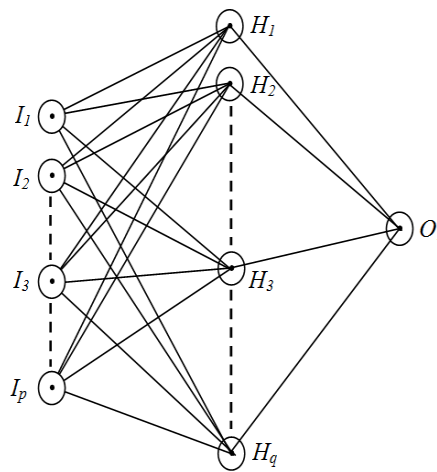


Fig. 6 A typical neural network model

recognition, adaptive learning, self-organization and real time operation. The back propagation algorithm has been used successfully for many structural engineering applications (Gupta *et al.* 2007, 2013, Kanwar *et al.* 2007, Mohammadhassani *et al.* 2013a, Chaudhary *et al.* 2007, 2014, Pendharkar *et al.* 2007, 2010, 2011, Tadesse *et al.* 2012) and is considered as one of the efficient algorithms in engineering applications (Hsu *et al.* 1993). One hidden layer is chosen and the number of neurons in the layer are decided in the learning process by trial and error.

It has been shown that the cracking at a joint affects the change in mid-span deflections of the first adjacent spans (Pendharkar *et al.* 2010). Therefore, the structural parameters which influence the change in the mid-span deflection of a span  $j$  are those which influence the cracking at the joints  $j$  and  $j + 1$ .

The parameters that influence cracking at joint  $j$  are:  $R_j^l, R_j^r, R_{j+1}^l, R_{j-1}^r, S_{j-1}/S_j, w_{j-1}/w_j, I^{cr}/I^{un}, t_0, Gr$  and that influence cracking at joint  $j + 1$  are:  $R_j^r, R_{j+1}^l, R_{j+1}^r, R_{j+2}^l, S_j/S_{j+1}, w_j/w_{j+1}, I^{cr}/I^{un}, t_0, Gr$ . Out of these eighteen parameters, five parameters are common i.e.,  $R_j^r, R_{j+1}^l, I^{cr}/I^{un}, t_0$  and  $Gr$ . Therefore, the neural network model for an internal span  $j$ , of a beam of a frame consists of thirteen input parameters,  $R_j^l, R_j^r, R_{j+1}^l, R_{j+1}^r, R_{j-1}^r, R_{j+2}^l, S_{j-1}/S_j, S_j/S_{j+1}, w_{j-1}/w_j, w_j/w_{j+1}, I^{cr}/I^{un}, t_0$  and  $Gr$  and one output parameter,  $\delta_j$ .

In case of neural network model for left external span ( $j = 1$ ), the input parameters,  $R_{j-1}^r, S_{j-1}/S_j, w_{j-1}/w_j$ , are absent and  $R_j^l$  is assigned a value equal to 10.0 (boundary condition). Similarly, for right external span ( $j = n$ ), the input parameters,  $R_{j+2}^l, S_j/S_{j+1}, w_j/w_{j+1}$  are absent and  $R_{j+1}^r$  is assigned a value equal to 10.0 (boundary condition). Thus, for two external spans, the input would consist of ten parameters each,  $R_1^l, R_1^r, R_2^r, R_2^l, R_3^l, S_1/S_2, w_1/w_2, I^{cr}/I^{un}, t_0, Gr$  (for left external span 1) and  $R_n^l, R_n^r, R_{n+1}^r, R_{n+1}^l, R_{n-1}^r, S_n/S_{n+1}, w_{n-1}/w_n, I^{cr}/I^{un}, t_0, Gr$  (for right external span  $n$ ), with corresponding output parameters being  $\delta_1$  and  $\delta_n$  respectively.

## 5. Training of neural network models

A beam of a frame may be considered as a continuous beam in which columns of upper and lower story provide rotational restraints (Fig. 7(a)) at the joints. This, in turn, may be represented by an equivalent single story frame (Fig. 7(b)) in which the columns provide the rotational restraints. Therefore, a single story frame has been used to generate training data sets (combination of different values of input parameters and the corresponding values of output parameters).

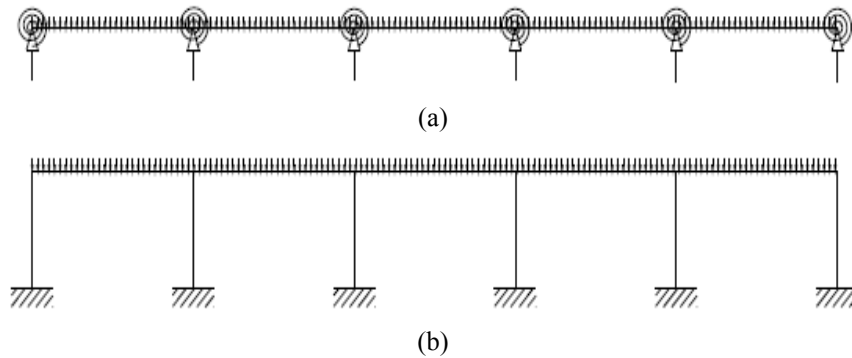


Fig. 7 (a) Continuous composite beam with rotational restraints, and (b) an equivalent single story frame

All the data sets are generated for a single story seven bay frame, henceforth designated as data generation frame. It is postulated that neural network models based on these training data sets are applicable for predicting  $\delta_j$  for any span of beams in frames of any number of stories.

Two neural network models, one each for external spans and internal spans and designated as Net-E, and Net-I, respectively, are trained. Input data sets are chosen to cover the entire practical range of parameters and sufficiently large number of values of each of the parameters. The training, validating, and testing data sets, typically for interior span, consist of thirteen input parameters and an output parameter. In order to have specified values of thirteen input parameters of a data set, an iterative procedure needs to be followed. The variables, for the data generation frame, in the hybrid analytical-numerical iterative procedure (Chaudhary *et al.* 2007b) are seven span lengths, seven corresponding loadings on the spans, cross-sectional properties, and grade of concrete and age of loading. The values of the variables are adjusted in such a manner that the specified values of thirteen input parameters are achieved. Similar exercise is done for exterior spans with ten input parameters.

Total 2,340 and 8,110 data sets, in the practical range of the parameters, could be generated for Net-E, and Net-I respectively. To bring all the input parameters and output parameter in the range 0.0 to 1.0, the input as well as the output parameters is divided by the normalization factors given in Table 1.

The training is carried out using the Stuttgart Neural Network Simulator (2012). For each network, 70% of the data sets are used for the training (as training patterns) whereas 15% of the data sets are used for the validating and the testing each. For this partitioning, 'hold out method' (Reich and Barai 1999), in which partitioning is done randomly, has been adopted. To train the neural network, back-propagation algorithm is adopted, which updates the weight and bias values to achieve a desired input-output relationship in each iteration that generates output values that are closer to the target values. For training, several trials are carried out with different numbers of

Table 1 Normalization factors

Network	Span	Input													Output
		$R_j^l$	$R_j^r$	$R_{j+1}^l$	$R_{j+1}^r$	$R_{j-1}^r$	$R_{j+2}^l$	$\frac{S_{j-1}}{S_j}$	$\frac{S_j}{S_{j+1}}$	$\frac{w_{j-1}}{w_j}$	$\frac{w_j}{w_{j+1}}$	$\frac{I^{cr}}{I^{un}}$	$t_o$ (days)	$Gr$ (N/mm <sup>2</sup> )	$\delta_j$
Net-E	Left external	10.05	4.05	4.05	4.05	-	4.05	-	4.05	-	4.05	1	22	41	5.5
	Right external	4.05	4.05	4.05	10.05	4.05	-	4.05	-	4.05	-	1	22	41	5.5
Net-I	Internal	4.05	4.05	4.05	4.05	10.05	10.05	4.05	4.05	4.05	4.05	1	22	41	26.0 (Bias +5.0)

Table 2 Configuration of networks, MSE,  $R_c^2$  and number of epochs

Network	Configuration	MSE			$R_c^2$			Epochs
		Training	Validating	Testing	Training	Validating	Testing	
Net-E	10-16-1	0.00106	0.00147	0.00253	0.946	0.939	0.937	45000
Net-I	13-16-1	0.00038	0.00062	0.00109	0.971	0.968	0.954	45000



neurons in the hidden layer. Care is taken that the mean square error for test results does not increase with the number of neurons in hidden layer or epochs (overtraining). The configurations of the two optimum networks (number of input parameters-number of neurons in hidden layer-number of output parameters) along with mean square error (MSE), square of coefficient of correlation ( $R_c^2$ ), and number of epochs are given in Table 2. The value of  $R_c^2$  for the networks is greater than 0.9 for training, validating, and testing data sets. The networks therefore have a good generalization capability.

## 6. Verification of neural networks models

Trained neural networks are verified for an example frame of 10 story-5 bay with a wide variation of input parameters (Fig. 8). These parameters are in different permutations than that used in training, validating, and testing. At all the floors, load intensity has been kept same as shown in the Fig. 8. The age of loading has been taken as 7 days. In the frame, 1000 mm wide and 70 mm thick concrete slab with M 32 grade of concrete and a steel I section with a cross-sectional area of  $5.14 \times 10^{-3} \text{ m}^2$ , moment of inertia of  $8.50 \times 10^{-5} \text{ m}^4$  about its major principle axis and depth of 305 mm, form the composite beams at all the floors. The slabs of composite beams of the frame have a reinforcement of area  $113 \text{ mm}^2$  placed at a distance of 15 mm from the top fibre. The columns consist of rolled steel sections with area of cross section as  $3.23 \times 10^{-3} \text{ m}^2$  and moment of inertia of  $2.36 \times 10^{-5} \text{ m}^4$ .

Results are compared for typical floor levels 5 and 10 for example frame EF. The network Net-E is used for external spans (spans 1 and 5), whereas network Net-I is used for internal spans (spans 2, 3 and 4). Table 3 shows the values of the input parameters for the external and internal spans of the example frame EF. As stated earlier, these parameters are in different permutations

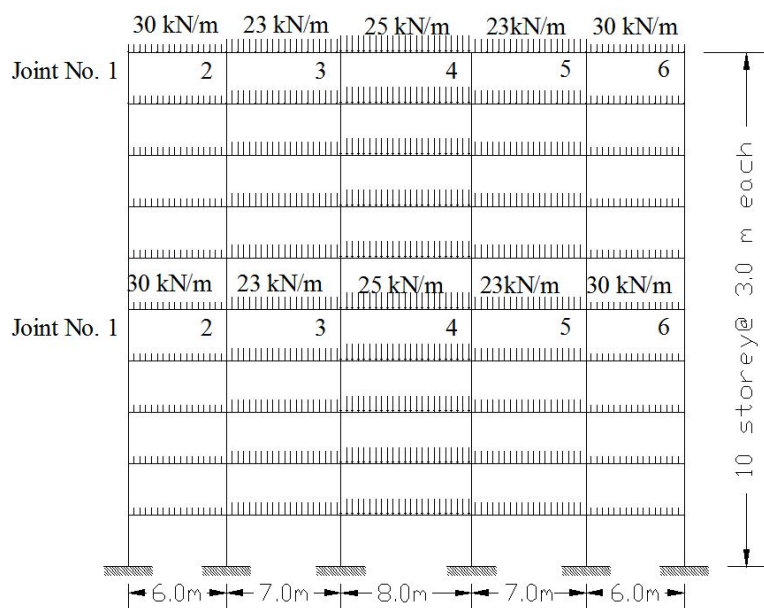


Fig. 8 An example frame (EF) of 10 story-5 bay

Table 3 Input parameters for an example frame EF

Network used	Floor level	Span No.	$R_j^l$	$R_j^r$	$R_{j+1}^l$	$R_{j+1}^r$	$R_{j-1}^r$	$R_{j+2}^l$	$\frac{S_{j-1}}{S_j}$	$\frac{S_j}{S_{j+1}}$	$\frac{w_{j-1}}{w_j}$	$\frac{w_j}{w_{j+1}}$	$\frac{I^{cr}}{I^{un}}$	$t_0$ (days)	$Gr$ (N/mm <sup>2</sup> )
Net-E	10th	1	0.195	0.172	0.148	0.045	-	0.995	-	0.288	-	0.322	0.463	0.318	0.781
		5	0.172	0.195	0.995	0.148	0.045	-	0.212	-	0.189	-	0.463	0.318	0.781
	5th	1	0.143	0.182	0.146	0.048	-	0.995	-	0.288	-	0.322	0.463	0.318	0.781
		5	0.182	0.143	0.995	0.146	0.048	-	0.212	-	0.189	-	0.463	0.318	0.781
Net-I	10th	2	0.148	0.112	0.114	0.114	0.172	0.195	0.288	0.282	0.322	0.227	0.463	0.318	0.781
		3	0.114	0.114	0.112	0.148	0.112	0.148	0.282	0.216	0.227	0.268	0.463	0.318	0.781
		4	0.112	0.148	0.172	0.195	0.114	0.114	0.216	0.212	0.268	0.189	0.463	0.318	0.781
	5th	2	0.143	0.182	0.146	0.118	0.195	0.172	0.288	0.282	0.322	0.227	0.463	0.318	0.781
		3	0.146	0.118	0.120	0.120	0.182	0.143	0.282	0.216	0.227	0.268	0.463	0.318	0.781
		4	0.120	0.120	0.118	0.146	0.118	0.146	0.216	0.212	0.268	0.189	0.463	0.318	0.781

Table 4 Comparison of inelastic mid-span deflections for example frame EF

Floor level	Span No.	$D^e$ (mm)	$D^i$ (mm)	
			Neural network	Hybrid procedure
10th	1	6.45	8.86	9.14
	2	3.54	5.76	5.31
	3	2.35	5.16	4.52
	4	3.54	5.57	5.31
	5	6.45	9.31	9.14
5th	1	5.03	7.50	7.25
	2	3.25	4.99	5.21
	3	2.43	5.11	4.69
	4	3.25	5.60	5.21
	5	6.45	8.86	9.14

than those used in training, validating, and testing. Table 4 shows the values of elastic deflection,  $D_j^e$ , and inelastic deflections,  $D_j^i$  obtained from the hybrid procedure and the neural networks. It is observed that in some cases (span 2-5 of 10th floor and span 1, 3, 4 of 5th floor level) higher values are predicted by the neural networks whereas in other cases (span 1 of 10th floor level and span 2, 5 of 5th floor level) lower values are predicted by the neural networks. It may be noted that the back propagation algorithm has been used for training which minimizes the root mean square error and therefore both types of errors are observed here. The root mean square percentage error in the prediction of mid-span inelastic deflections is 2.54% for external spans and 3.38% for internal spans which is acceptable for practical design. This shows the efficacy of developed neural network models for moderately high frames with any number of spans and stories.

In practice, span/deflection ratio is limited to the range between 250 and 350. For span having a lower value of span/deflection ratio, percentage error in prediction of mid-span inelastic deflection

is small. The maximum error for a span having span/deflection ratio of 931 (span 1, 10th floor) is 3.06%, whereas, the maximum error for a span having span/deflection ratio of 3400 (span 3, 10th floor) is 14.16%.

## 7. Sensitivity analysis

Sensitivity studies are carried out using the developed neural networks. These studies show the influence of variations of input parameters on the output parameters.

For the sensitivity analysis, one parameter (the parameter under consideration) is varied at a time while keeping the other parameters constant equal to their median values. For an internal span, the variations of the output parameter  $\delta_j$  with the different input parameters are presented below.

### 7.1 Effect of $R_j^r$ and $R_{j+1}^l$

Figs. 9-10 show variation of  $\delta_j$  with  $R_j^r$  and  $R_{j+1}^l$  respectively. The range  $R_j^r = R_{j+1}^l = 1.0 - 4.0$  indicates absence of cracking. The increase in the value of  $R_j^r$  and  $R_{j+1}^l$  (larger value of  $R_j^r$  and  $R_{j+1}^l$  indicates smaller applied loading) means less effect of creep and thereby lesser time-dependent change in deflection (as the other component shrinkage is independent of load).

In the range,  $R_j^r = R_{j+1}^l = 0.25 - 1.0$ , cracking of concrete occurs in the end portions of the beams. The increase in the value of  $R_j^r$  and  $R_{j+1}^l$  means lesser cracking and thereby lesser change in instantaneous deflections. The large uncracked portions means larger portion is subjected to creep and shrinkage however, the stiffer (uncracked) section leads to lower change in deflections and also lower loads/moments lead to lower time-dependent change in deflections due to creep.

Therefore, for the entire range  $R_j^r = R_{j+1}^l = 0.25 - 4.0$ , the value of  $\delta_j$  is found to decrease with increase in value of  $R_j^r$  and  $R_{j+1}^l$ . The value of  $\delta_j$  is insignificant at  $R_j^r = R_{j+1}^l = 4.0$  as the change in mid-span deflection is mostly due to shrinkage (instantaneous change in deflection being zero due to absence of cracking and change due to creep being very small due to lower moments) which is small in comparison to  $D_j^{eq} = M^{cr} l_j^2 / 32EI$ .

### 7.2 Effect of $R_j^l$ and $R_{j+1}^r$

The variations of  $\delta_j$  with  $R_j^l$  and  $R_{j+1}^r$  are shown in Figs. 11-12 respectively. The effect of these

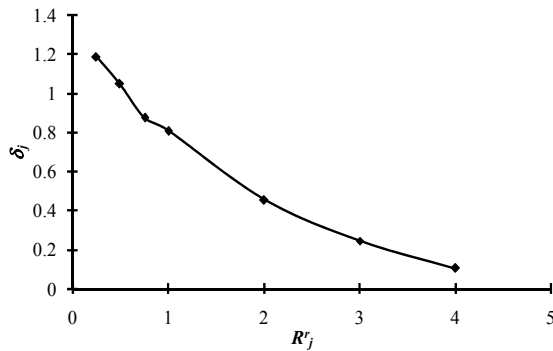


Fig. 9 Variation of  $\delta_j$  with  $R_j^r$

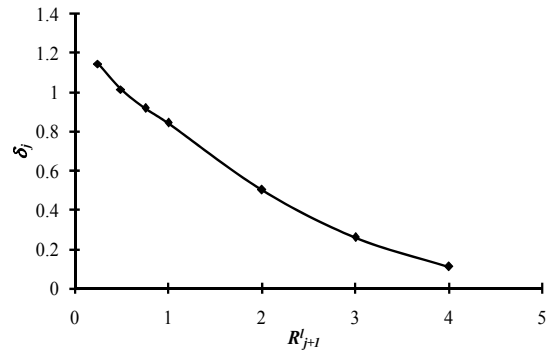
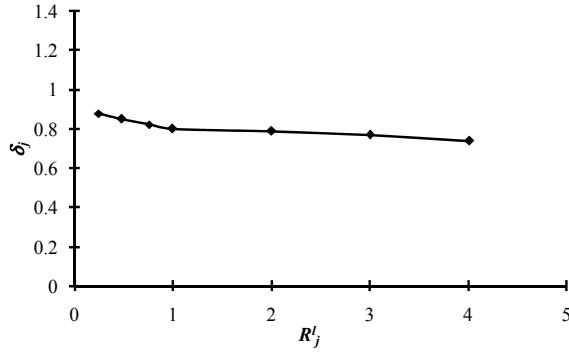
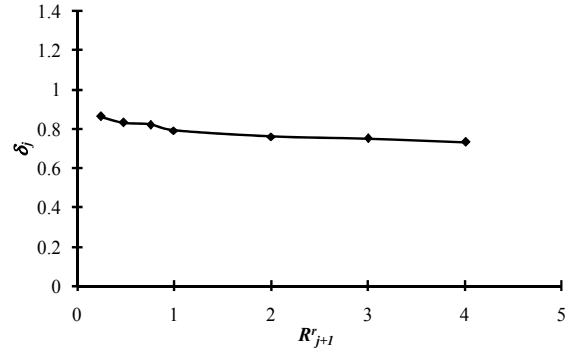
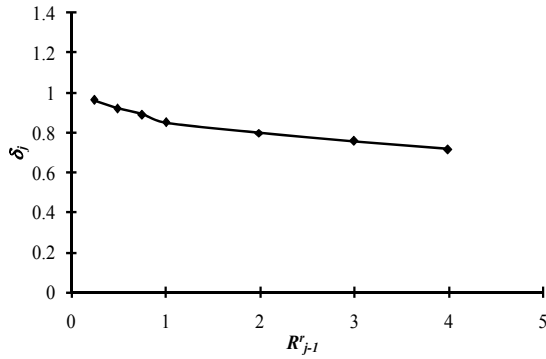
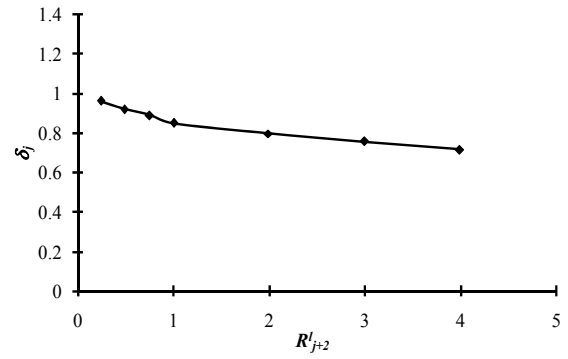
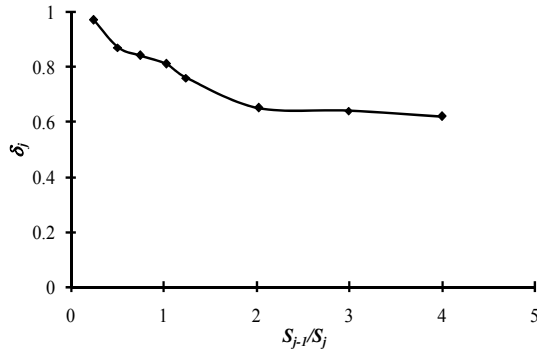
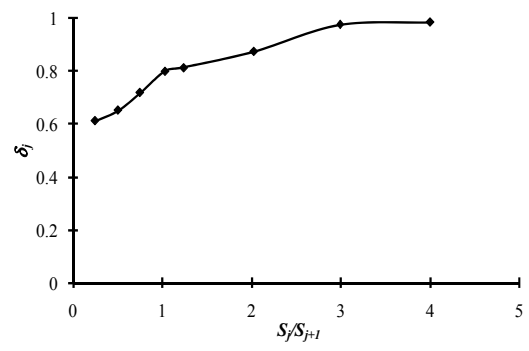


Fig. 10 Variation of  $\delta_j$  with  $R_{j+1}^l$

Fig. 11 Variation of  $\delta_j$  with  $R_j^l$ Fig. 12 Variation of  $\delta_j$  with  $R_{j+1}^r$ Fig. 13 Variation of  $\delta_j$  with  $R_{j-1}^r$ Fig. 14 Variation of  $\delta_j$  with  $R_{j+2}^l$ Fig. 15 Variation of  $\delta_j$  with  $S_{j-1}/S_j$ Fig. 16 Variation of  $\delta_j$  with  $S_j/S_{j+1}$ 

parameters is found to be small. The higher values of  $R_j^l$  and  $R_{j+1}^r$  will mean less redistribution of moments to span  $j$  leading to less cracking and thereby less change in instantaneous deflections of span  $j$ . A marginal decrease is therefore observed in value of  $\delta_j$  with increase in value of  $R_j^l$  and  $R_{j+1}^r$ .

### 7.3 Effect of $R_{j-1}^r$ and $R_{j+2}^l$

Figs. 13-14 show variation of  $\delta_j$  with  $R_{j-1}^r$  and  $R_{j+2}^l$  respectively. The effect of these parameters

is found to be similar to  $R_j^l$  and  $R_{j+1}^r$  but smaller due to distance from the span under consideration.

#### 7.4 Effect of $S_{j-1}/S_j$ and $S_j/S_{j+1}$

The variations of  $\delta_j$  with  $S_{j-1}/S_j$  and  $S_j/S_{j+1}$  are shown in Figs. 15-16 respectively. The decrease in values of  $\delta_j$  is observed with increase in value of  $S_{j-1}/S_j$  and decrease in value of  $S_j/S_{j+1}$  due to higher restrained of side spans on change in deflection. The effect is not very significant. The cracking moment ratios  $R_{j-1}^r, R_j^l, R_j^r, R_{j+1}^l, R_{j+1}^r$  and  $R_{j+1}^l$  are kept constant as  $S_{j-1}/S_j$  and  $S_j/S_{j+1}$  are varied. Thus, with the elastic moments at the joints remaining constant, differing elastic moment distributions in spans  $j-1$  and  $j$  resulting from different values of  $S_{j-1}/S_j$  and  $S_j/S_{j+1}$  would not contribute significantly to  $\delta_j$ .

#### 7.5 Effect of $w_{j-1}/w_j$ and $w_j/w_{j+1}$

Figs. 17-18 show the variation of  $\delta_j$  with  $w_{j-1}/w_j$  and  $w_j/w_{j+1}$  respectively. Again, as observed for  $S_{j-1}/S_j$  and  $S_j/S_{j+1}$ , the decrease in values of  $\delta_j$  is observed with increase in value of  $w_{j-1}/w_j$  and decrease in value of  $w_j/w_{j+1}$ , though the decreases is not very significant.

#### 7.6 Effect of $I^r/I^u$

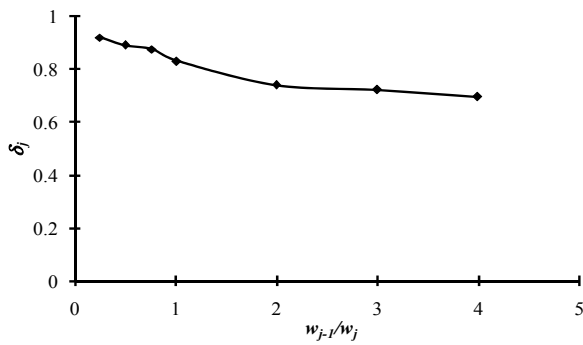


Fig. 17 Variation of  $\delta_j$  with  $w_{j-1}/w_j$

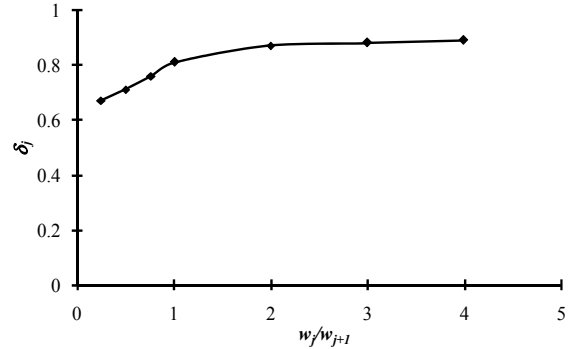


Fig. 18 Variation of  $\delta_j$  with  $w_j/w_{j+1}$

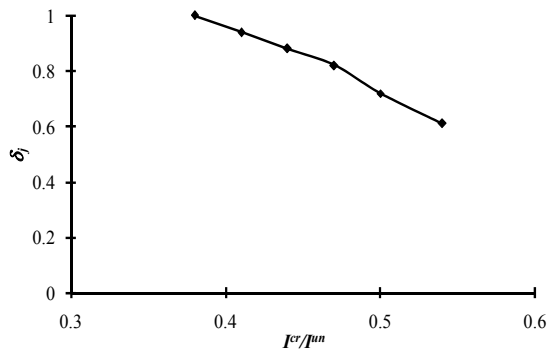


Fig. 19 Variation of  $\delta_j$  with  $I^r/I^u$

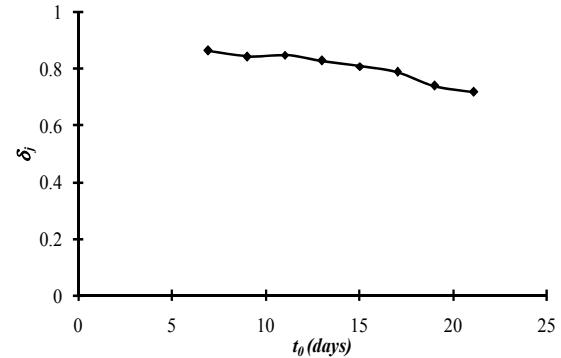
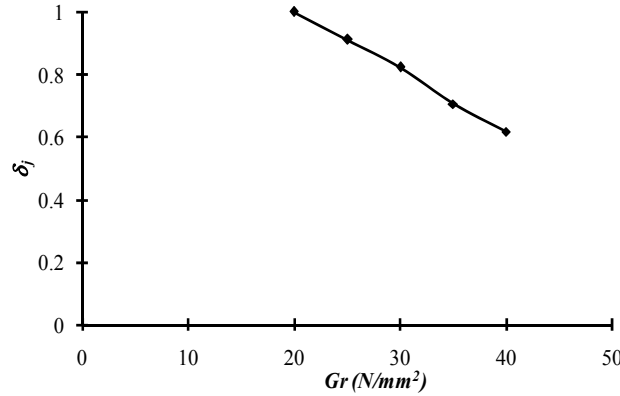


Fig. 20 Variation of  $\delta_j$  with  $t_0$

Fig. 21 Variation of  $\delta_j$  with  $Gr$ 

The stiffness of a composite section,  $I^{un}$  reduces to that of a steel section,  $I^{cr}$  on cracking, which leads to redistribution of forces. The variation of  $\delta_j$  with  $I^{cr} / I^{un}$  is shown in Fig. 19. Increasing values of  $I^{cr} / I^{un}$  result in smaller effect of a instantaneous cracking due to lesser change in stiffness on cracking and therefore in smaller values of  $\delta_j$ .

#### 7.7 Effect of $t_0$

The cracking at support and thus the mid-span deflections of the adjacent spans may vary with the age of loading,  $t_0$ . The variation of  $\delta_j$  with  $t_0$  for an internal span of a frame is shown in Fig. 20. With the increase in  $t_0$ , the tensile strength of the concrete increases and the creep coefficient and the shrinkage strain decrease, therefore  $\delta_j$  is found to decrease with increase in  $t_0$ .

#### 7.8 Effect of $Gr$

The changes in mid-span deflections due to cracking and time effects depend upon the grade of concrete,  $Gr$ . Fig. 21 shows the variation of  $\delta_j$  with  $Gr$  for an internal span of a frame where it is observed that there is a reduction in  $\delta_j$  with the increase in  $Gr$ . With the increase in  $Gr$ , the tensile strength of the concrete increases and the creep coefficient and the shrinkage strain decrease. The variation of  $\delta_j$  with  $Gr$  is therefore similar to that observed for  $t_0$ .

### 8. Conclusions

A methodology has been presented for rapid prediction of inelastic deflections, at preliminary design stage, in large steel-concrete composite frames, from elastic deflections by using the neural network models. The methodology has been demonstrated for moderately high composite frames (where differential settlement of columns is not large enough to cause sagging at the ends of the beams) by developing two neural network models. The two models, Net-E and Net-I, are applicable for exterior spans and interior spans respectively. The models have been verified with an example frame. A sensitivity analysis is also carried out to identify the important parameters affecting the output parameter. Following are the important findings of the study:

- The most significant parameters affecting the value of  $\delta_j$  are  $R_j^l$  and  $R_{j+1}^r$ .
- The developed neural network models can predict the inelastic deflections with reasonable accuracy from the elastic deflections, which in turn, can be obtained from any of the readily available software. The computational effort required is a fraction of that required for the available methods.
- The overall root mean square percentage error in the prediction of deflection for the example frame, considered for validation is about 2.54% and 3.38% for exterior spans and interior spans respectively, which is acceptable for practical design.
- The neural networks are applicable for moderately high composite frames of any number of spans and stories.

The methodology can be used for developing the neural networks for rapid prediction of inelastic deflections in high rise composite frames also where the effect of axial shortening of the columns is significant. For the data generation, the high rise frames can be used instead of single story frame. Further, the slip between concrete slab and steel beam may be incorporated in future studies.

## References

- Bazant, Z.P. (1972), "Prediction of concrete creep-effects using age adjusted effective modulus method", *ACI J.*, **69**(4), 212-217.
- Chaudhary, S., Pendharkar, U. and Nagpal, A.K. (2007a), "Bending moment prediction for continuous composite beams by neural networks", *Adv. Struct. Eng.*, **10**(4), 439-454.
- Chaudhary, S., Pendharkar, U. and Nagpal, A.K. (2007b), "Hybrid procedure for cracking and time-dependent effects in composite frames at service load", *J. Struct. Eng.*, **133**(2), 166-175.
- Chaudhary, S., Pendharkar, U. and Nagpal, A.K. (2007c), "An analytical-numerical procedure for cracking and time-dependent effects in continuous composite beams under service load", *Steel Comp. Struct., Int. J.*, **7**(3), 219-240.
- Chaudhary, S., Pendharkar, U., Patel, K.A. and Nagpal, A.K. (2014), "Neural networks for deflections in continuous composite beams considering concrete cracking", *Iran. J. Sci. Technol., Trans. Civil Eng.*, **38**(C1+), 205-221.
- Comité Euro International du Béton-Fédération International de la Précontrainte (CEB-FIP) (1993), Model code for concrete structures, Thomas Telford, London, UK.
- Feng, Q.M., Kim, D.K., Yi, J.H. and Chen, Y. (2004), "Baseline models for bridge performance monitoring", *J. Eng. Mech.*, **130**(5), 562-569.
- Ghali, A., Favre, R. and Elbadry, M. (2002), *Concrete Structures: Stresses and Deformations*, (3rd Ed.), Spon Press, London, UK.
- Gholizadeh, S. and Salajegheh, E. (2010), "Optimal seismic design of steel structures by an efficient soft computing based algorithm", *J. Constr. Steel Res.*, **66**(1), 85-95.
- Gupta, V.K., Kwatra, N. and Ray, S. (2007), "Artificial neural network modeling of creep behavior in a rotating composite disc", *Eng. Computation.*, **24**(2), 151-164.
- Gupta, R.K., Patel, K.A., Chaudhary, S. and Nagpal, A.K. (2013), "Closed form solution for deflection of flexible composite bridges", *Procedia Eng.*, **51**, 75-83.
- Hsu, D.S., Yeh, I.C. and Lian, W.T. (1993), "Artificial neural damage detection of existing structure", *Proceedings of the 3rd ROC and Japan Seminar on Natural Hazards Mitigation*, Tainan, Taiwan, November, pp. 423-436.
- Kanwar, V., Kwatra, N. and Aggarwal, P. (2007), "Damage detection for framed RCC buildings using ANN

- modeling", *Int. J. Damage Mech.*, **16**(4), 457-472.
- Kaloop, M.R. and Kim, D. (2014), "GPS-structural health monitoring of a long span bridge using neural network adaptive filter", *Survey Review*, **16**(334), 7-14.
- Kawamura, K., Miyamoto, A., Frangopol, D.M. and Abe, M. (2004), "Performance evaluation system for main reinforced concrete girders of existing bridges", *Transport. Res. Rec.*, **1866**, 67-78.
- Kim, D.K., Kim, D.H., Cui, J., Seo, H.Y. and Lee, Y.H. (2009), "Iterative neural network strategy for static model identification of an FRP deck", *Steel Comp. Struct., Int. J.*, **9**(5), 445-455.
- Kwatra, N., Godbole, P.N. and Krishna, P. (2002), "Application of artificial neural network for determination of wind induced pressures on gable roof", *Wind Struct.*, **5**(1), 1-14.
- Min, J., Park, S., Yun, C.B., Lee, C.G. and Lee, C. (2012), "Impedance-based structural health monitoring incorporating neural network technique for identification of damage type and severity", *Eng. Struct.*, **39**, 210-220.
- Mohammadhassani, M., Nezamabadi-Pour, H., Jumaat, M.Z., Jameel, M. and Arumugam, A.M.S. (2013a), "Application of artificial neural networks (ANNs) and linear regressions (LR) to predict the deflection of concrete deep beams", *Comput. Concrete*, **11**(3), 237-252.
- Mohammadhassani, M., Nezamabadi-Pour, H., Jumaat, M.Z., Jameel, M., Hakim, S.J.S. and Zargar, M. (2013b), "Application of the ANFIS model in deflection prediction of concrete deep beam", *Struc. Eng. Mech., Int. J.*, **45**(3), 319-332.
- Pendharkar, U., Chaudhary, S. and Nagpal, A.K. (2007), "Neural network for bending moment in continuous composite beams considering cracking and time effects in concrete", *Eng. Struct.*, **29**(9), 2069-2079.
- Pendharkar, U., Chaudhary, S. and Nagpal, A.K. (2010), "Neural networks for inelastic mid-span deflections in continuous composite beams", *Struc. Eng. Mech., Int. J.*, **36**(2), 165-179.
- Pendharkar, U., Chaudhary, S. and Nagpal, A.K. (2011), "Prediction of moments in composite frames considering cracking and time effects using neural network models", *Struc. Eng. Mech., Int. J.*, **39**(2), 267-285.
- Reich, Y. and Barai, S.V. (1999), "Evaluating machine learning models for engineering problems", *Artif. Intell. Eng.*, **13**(3), 257-272.
- Shahin, M. and Elchanakani, M. (2008), "Neural networks for ultimate pure bending of steel circular tubes", *J. Constr. Steel Res.*, **64**(6), 624-633.
- Sharma, R.K., Maru, S. and Nagpal, A.K. (2003), "Effect of creep and shrinkage in a class of composite frame-shear wall systems", *Steel Comp. Struct., Int. J.*, **3**(5), 333-348.
- Stuttgart Neural Network Simulator (SNNS) user manual (1998), University of Stuttgart: Institute For Parallel and Distributed High Performance Systems (IPVR), Version 4.2, Accessed on December 27, 2012; Available at: <http://www-ra.informatik.uni-tuebingen.de/SNNS/>
- Tadesse, Z., Patel, K.A., Chaudhary, S. and Nagpal, A.K. (2012), "Neural networks for prediction of deflection in composite bridges", *J. Constr. Steel Res.*, **68**(1), 138-149.
- Uddin, M.A., Jameel, M., Razak, H.A. and Islam, A.B.M. (2012), "Response prediction of offshore floating structure using artificial neural network", *Adv. Sci. Lett.*, **14**(1), 186-189.
- Wang, W.W., Dai, J.G., Guo, L. and Huang, C.K. (2011), "Long-term behavior of prestressed old-new concrete composites beams", *J. Bridge Eng.*, **16**(2), 275-285.



**Notations**

$D$	: mid-span deflection;
$E$	: modulus of elasticity of concrete;
$Gr$	: grade of concrete;
$H$	: hidden neuron;
$I$	: Input parameter;
$I^{nn}$	: transformed moment of inertia of composite section
$I^{cr}$	: transformed moment of inertia of steel section and reinforcement;
$M$	: bending moment;
$O_1$	: output parameter;
$R_{j+2}^l, R_j^l, R_{j+1}^l,$ $R_{j-1}^r, R_j^r, R_{j+1}^r,$	: cracking moment ratios;
$RH$	: relative humidity;
$S$	: Stiffness;
$L$	: span length;
$N$	: number of spans/bays;
$t_0$	: age of loading;
$w$	: uniformly distributed load;
$\delta$	: inelastic deflection ratio.

**Subscript**

$j$	: support or span number;
$p$	: number of input parameters;
$q$	: number of hidden neurons.

**Superscript**

$cr$	: cracking;
$e$	: elastic;
$i$	: inelastic;
$l$	: left side of a joint;
$r$	: right side of a joint.